

Finite Element Method Based Modeling for Cutting Force Predication in Orthogonal Cutting Process

A Hatem Ali^{1*}, B Tarek M El Hossainy² and CM Abd-Rabou²Modern Academy for Engineering and Technology, Cairo, Egypt¹Department of Mechanical Design and Production, Cairo University, Cairo, Egypt²

Abstract: This paper deals with plane strain modeling using finite element method (FEM) in orthogonal cutting process. The main objective is to simulate the cutting process using finite element program code (Abaqus /CAE) and extract the cutting force – tangential force- due to its vital role in machining. The experimental work includes dynamometer calibration and using it during orthogonal cutting of steel pipes by tungsten carbide tool-tip on center lathe machine to indicate the cutting force. Also, this paper presents a comparative study between two simulation methods; Lagrangian method and Arbitrary Lagrangian- Eulerian (ALE) method. The comparative study discusses the accuracy, stability and chip form of the extracted results from the two models comparing with the experimental data. Johnson-Cook (J-C) model is used for the finite element model to define the plastic and damage properties of the simulated materials.

Keywords: Plane strain, Finite element method (FEM), Orthogonal cutting, Lagrangian, Arbitrary lagranigan-eulerian , Johnson-Cook

I. INTRODUCTION

Nowadays, machining processes are almost the most important mechanical processes in industry as most of the products get the final shape and size by machining. Therefore, machining has a great interest for the researchers. Finite Element Method (FEM) is a numerical method, which is used to solve engineering, mathematical and physics problems. Therefore, the utilization of FEM in machining such as orthogonal cutting give great advantage for simulation the cutting processes and solution of many problems related to metal cutting. Researchers always have the interest to apply the finite element modeling in machining to achieve the powerful of the finite element in studying the complex problems related to machining in less time and with less effort than the time and effort that should be done by experimental work to study the same problem.

Orthogonal Cutting

In machining, there are two types of metal cutting: orthogonal cutting and oblique cutting.. The main difference between them is the chip flow direction on the tool face. When the chip flows along orthogonal plane perpendicular to the cutting edge, the cutting process is called orthogonal cutting process and when the chip flow deviates from that orthogonal plane that's called oblique cutting. This paper presents pure orthogonal cutting which is the case of orthogonal cutting, moreover the tool cutting edge is perpendicular to the workpiece ($\lambda=90^\circ$) and the tool geometry with rake angle equal to zero ($\sigma=0^\circ$). Reduction the length of steel pipe using center lathe machine is an example for pure orthogonal cutting as shown in Fig. 1.

International Journal of Innovative Research in Science, Engineering and Technology

(An ISO 3297: 2007 Certified Organization)

Vol. 6, Issue 8, August 2017

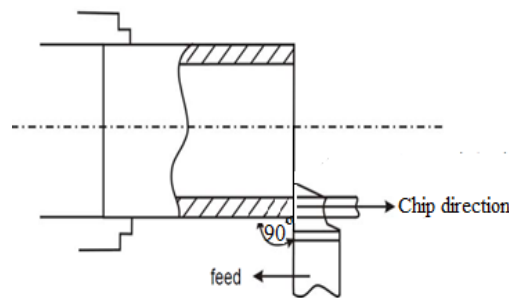


Fig. 1. Pure orthogonal cutting (pipe turning).

Cutting Forces in Case of Pipe Length Reduction Turning

Pipe length reduction is a two dimensional action. It means that there is only two components of forces are existed, the tangential force F_t and the axial force F_a . Thus, the resultant force is,

$$F = \sqrt{F_a^2 + F_t^2}$$

As shown in Fig. 2 in the case of reducing the length of a pipe by turning, the pipe is hollow and there is no resistance or material acts on tool in the radial direction resulting in no radial force ($F_r=0$).

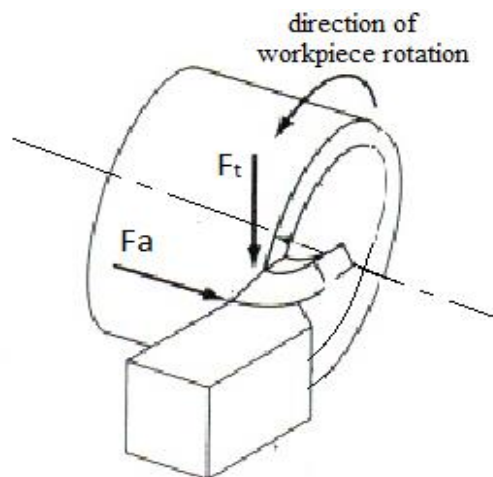


Fig. 2. Cutting forces in pipe length reduction.

Adaptive Meshing

Finite element method has three methods to describe the motion of the model: Lagrangian, Eulerian and Arbitrary Lagrangian-Eulerian (ALE) method. In Lagrangian method, the mesh grid moves with the material points. In Eulerian method, the mesh grid is fixed in position and the material moves through the mesh grid. Arbitrary Lagrangian-Eulerian allows the material to flow with the mesh grid in arbitrary way trying to conserve the initial mesh grading or to improve the aspect ratio of the elements. ALE method is a combination of Lagrangian method and Eulerian method and overcomes the disadvantages of both methods especially in machining processes simulation [1]. This method follows adaptive meshing technique, by the meaning that after number of time increments, the ALE technique allows the current mesh to be remeshed by reallocating the nodes to avoid the excessive distortions of the elements to be occurred. Thus, the solution variables (stress, strain, temperature, etc.) are also remapped to this reformed mesh [2].

International Journal of Innovative Research in Science, Engineering and Technology

(An ISO 3297: 2007 Certified Organization)

Vol. 6, Issue 8, August 2017

Fig. 3 shows the difference between the three methods. One of the common problems in the simulation of machining process is that the occurred excessive distortion in elements due to large deformation in workpiece and high strain rate. Thus, adaptive mesh with arbitrary Lagrangian-Eulerian method is recommended to be used in FE programs to solve and handle with this problem.

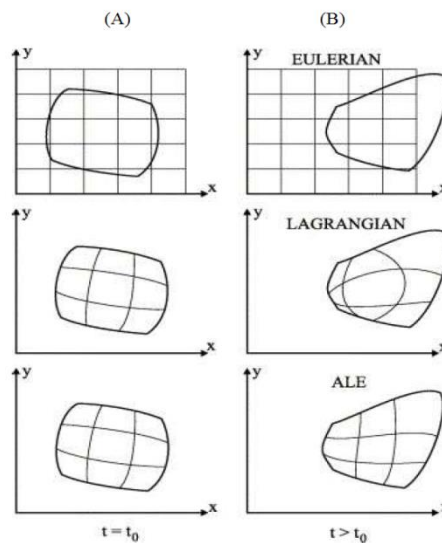


Fig. 3. Difference between Lagrangian, Eulerian and ALE method (A) At the beginning of simulation at initial time (t_0). (B) After running simulation with time period (t) [3].

Johnson-Cook Material Model

There are many constitutive models describes the material behavior in finite element modeling such as Oxley model, Johnson-Cook model and Zeirilli and Armstrong. Comparative studies are presented in literature between the three models to discuss the difference of utilizing them in machining simulation [4]. However, the most commonly used is Johnson-Cook (J-C) constitutive model as it is also available in most of the commercial FE programs. Johnson-Cook has two models describing the material behavior; Equation (1) describes the plastic behavior of the material deformation, and equation (2) describes the failure behavior of the material. Both of these two equations are implemented in Abaqus /CAE program by defining their parameters into the program to define the material behavior for the simulation model.

$$\bar{\sigma} = (A + \bar{\epsilon}^n) \left[1 + C \ln \left(\frac{\dot{\epsilon}^{pl}}{\dot{\epsilon}_0} \right) \right] \left[1 - \left(\frac{T - T_{room}}{T_m - T_{room}} \right)^m \right] \quad (1)$$

Where, $\bar{\sigma}$ is the equivalent plastic stress (MPa) , $\bar{\epsilon}$ is the equivalent plastic strain, $\dot{\epsilon}^{pl}$ is the equivalent plastic strain rate, $\dot{\epsilon}_0$ is the referenced equivalent plastic strain rate, T is the temperature ($^{\circ}\text{C}$), T_m is the work material melting temperature ($^{\circ}\text{C}$), T_{room} is room temperature ($^{\circ}\text{C}$), A, B, C, m and n are parameters of material.

$$\bar{\epsilon}_f^{pl} = \left[D_1 + D_2 \exp D_3 \left(\frac{P}{\sigma} \right) \right] \left[1 + D_4 \ln \left(\frac{\dot{\epsilon}^{pl}}{\dot{\epsilon}_0} \right) \right] \left[1 + D_5 \frac{T - T_{room}}{T_{melt} - T_{room}} \right] \quad (2)$$

Where, $\bar{\epsilon}_f^{pl}$ is the critical strain at failure, P is the hydrostatic pressure (MPa), σ is the effective (undamaged) stress (MPa), D_1 , D_2 , D_3 , D_4 and D_5 are the failure parameters of the material, and they are determined from experiments and mechanical tests.

International Journal of Innovative Research in Science, Engineering and Technology

(An ISO 3297: 2007 Certified Organization)

Vol. 6, Issue 8, August 2017

Experimental Work

The experimental work included two steps; first step is the calibration of the dynamometer device to indicate the cutting force during the cutting process. The calibration steps are held by using Tension-Compression machine (WOLBERT AMSLER testing machine – 100 kN maximum load) as shown in Fig. 4.



Fig. 4. Dynamometer calibration set up.

Calibration steps

1. Connecting the dynamometer device with the laptop.
2. Adjusting the tool into the dynamometer holder in suitable position for calibrating the strain gauges that will indicate the tangential force –cutting force- value in the cutting process. The applied force direction must be perpendicular to the tool edge as shown in Fig. 5.
3. Clamping the dynamometer holder on the tension-compression machine table.

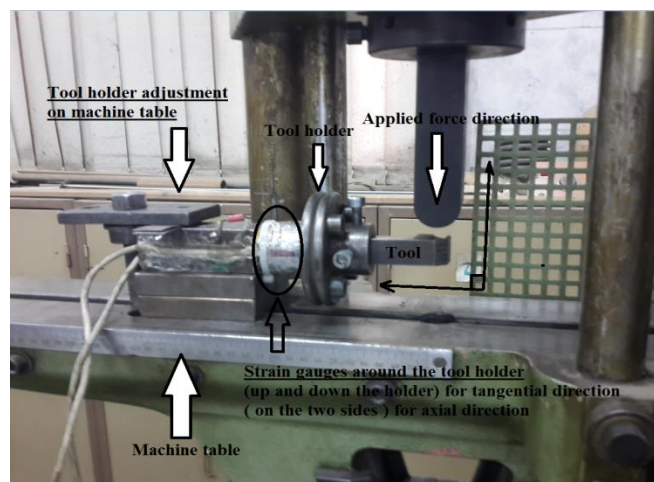


Fig. 5. Clamping position for calibration the dynamometer tangential direction.

International Journal of Innovative Research in Science, Engineering and Technology

(An ISO 3297: 2007 Certified Organization)

Vol. 6, Issue 8, August 2017

4. Applying the force on the tool head.
5. Recording ten readings of dynamometer output for ten known forces values (50, 100, 150, 200, 250, 300, 350, 400, 450 and 500 Newton).
6. Recording the forces values and voltage readings in excel sheet to plot them and extract the equation of tangential force direction.

The Second Part in experimental work is the machining process which is orthogonal cutting of steel pipes ASTM A106 on center lathe machine by using single point tool with tungsten carbide tip at different feed rates (0.12, 0.15, 0.18, 0.2, 0.22 and 0.26 mm/rev) and constant velocity = 60 m/min. It is advisable to choose applicable cutting case, thus the choice of workpiece material, tool geometry and cutting conditions was chosen from standard data handbooks [5-7]. Table 1 shows the cutting parameters used for the cutting process.

Table 1. The cutting parameters.

Materials	Velocity	Feed rate	Tool angles
Tool : Tungsten Carbide (uncoated) Workpiece : low carbon steel pipe	60 m./min.	0.12, 0.15, 0.18 , 0.2, 0.22 and 0.26 mm./rev.	Rake angle=0° Relief angle=10° Approach angle=90° Inclination angle=0°

Simulation Work

The simulation work included the modeling of the orthogonal cutting process and applying the finite element method by using ABAQUS /CAE program.

Model Formulation

In part module ABAQUS/CAE program, the tool and workpiece are modeled in 2D planar as deformable parts. Small portions were enough to model the tool and workpiece as shown in Fig. 6. Two partitioning lines are made in workpiece model, one with depth equal the feed value and the other line with depth more than the maximum feed value. The first line is made to help in tool penetration through workpiece model and separate the chip part with less simulation running time and the second line is made to allow making dense mesh region below the region of tool penetration in workpiece to extract accurate results from that region [8,9].

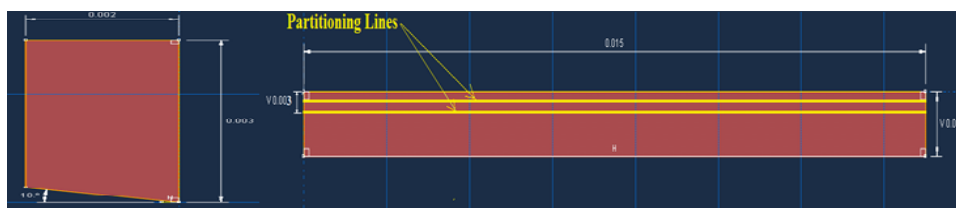


Fig. 6. Tool and workpiece model dimension a. tool sketch b. Workpiece sketch.

International Journal of Innovative Research in Science, Engineering and Technology

(An ISO 3297: 2007 Certified Organization)

Vol. 6, Issue 8, August 2017

In assembly module, the tool and workpiece are assembled together and a step time is calculated for the model by dividing the workpiece displacement over the cutting velocity (step time=length/ velocity) and then it is implemented into the program step module. The cutting velocity -60 m/min- is defined as boundary condition for the workpiece but the tool is defined as totally fixed in position as shown in Fig. 7.

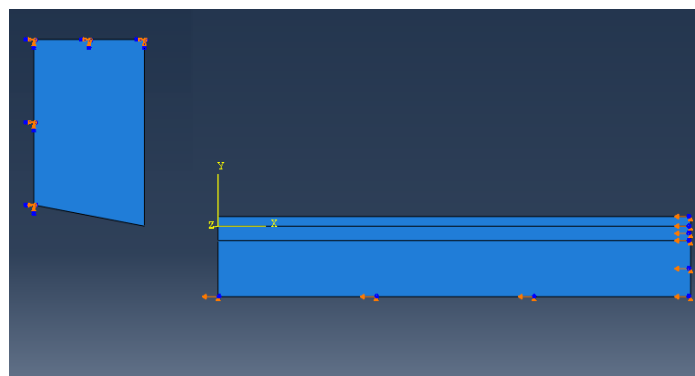


Fig. 7. Boundary conditions for tool and workpiece.

Contact pairs must be defined with friction between the tool surfaces and the upper part of workpiece as node region as shown in Fig. 8.

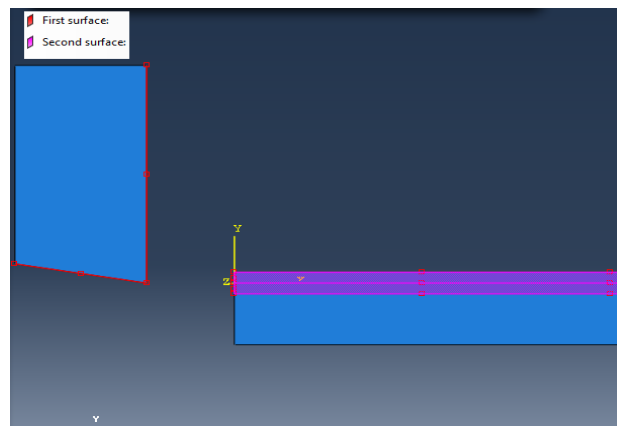


Fig. 8. Contact pairs definition.

II. MATERIALS DEFINITIONS

In material definition module, the parameters that describe the tool and workpiece material in elastic, plastic and failure behavior are implemented in the program as following (Tables 2-5):

Tool is defined as tungsten carbide material. The tungsten carbide properties are:

- Density=15630 kg/m³
- Elastic properties; Young's Modulus=550 GPa , and Poisson's ratio=0.234

International Journal of Innovative Research in Science, Engineering and Technology

(An ISO 3297: 2007 Certified Organization)

Vol. 6, Issue 8, August 2017

- Plastic properties

Table 2. Carbide tungsten plastic model constants [9].

Yield Stress (Pa)	Effective plain strain
419530000	0
1696900000	0.000263
2675500000	0.00097364
3376500000	0.002107
3858200000	0.003574
4178000000	0.005287
4382200000	0.007176
450480000	0.00919
4570100000	0.01129
4595500000	0.013452
4597300000	0.014279
4597300000	0.1

- Johnson-Cook damage model

Table 3. Carbide tungsten damage model constants [9].

D1	D2	D3	D4	D5
0	0.0107	-1.67	0	0

Workpiece material is defined as steel ASTM A36, the steel ASTM A36 properties are:

- Density=7800 kg/m³
- Elastic properties; Young's Modulus=200 GPa , and Poisson's ratio=0.26
- Plastic properties

Table 4. Steel A36 plastic Johnson-Cook model constants [10].

A (MPa)	B (MPa)	C	M	N	Reference strain rate
286.1	500.1	0.022	0.917	0.2282	1

- Johnson-Cook damage model

International Journal of Innovative Research in Science, Engineering and Technology

(An ISO 3297: 2007 Certified Organization)

Vol. 6, Issue 8, August 2017

Table 5. Steel A36 damage model constants [10].

D1	D2	D3	D4	D5
0.4	1.11	-1.9	0.0096	0

Model Meshing

In the mesh module, a 4-node bilinear plane strain quadrilateral, reduced integration, and automatic hourglass control (CPE4R) element type was assigned to tool and workpiece models from the element library. The number of elements used in the tool and workpiece meshing effects on the simulation accuracy. Series of program runs was carried out to determine the appropriate number of elements of tool and workpiece for each feed rate value that gives suitable simulation of chip forming. The number of elements that gave suitable modeling, stable force results and close results to experimental work was 2600 element for workpiece and 200 elements for tool. All feed rates are simulated by that number of elements but with dense mesh in the penetration zone as in Fig. 9 to give accurate results. [10].

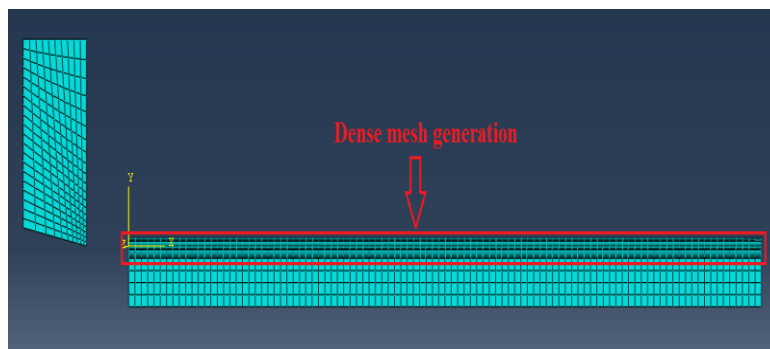


Fig. 9. Model mesh generation.

Adaptive Meshing

Arbitrary Lagrangian-Eulerian (ALE) or Adaptive mesh technique is applied to the model through the step module. In the step module, all requirements of adaptive mesh method such as the ALE adaptive mesh domain – Fig. 10, constraints and control are defined.

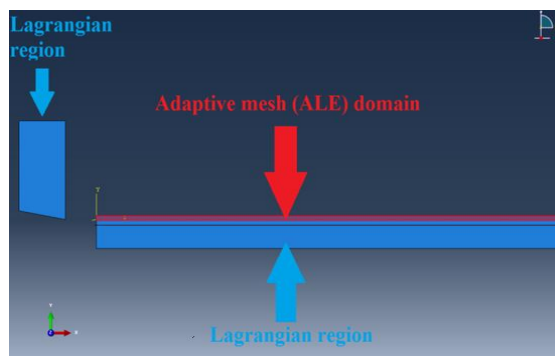


Fig. 10. ALE and Lagrangian region for the model.

International Journal of Innovative Research in Science, Engineering and Technology

(An ISO 3297: 2007 Certified Organization)

Vol. 6, Issue 8, August 2017

III. RESULTS AND DISCUSSION

Experimental Results

Table 6 shows the calibration results of the dynamometer device in the tangential direction. The chart in Fig. 11 is established for the calibration data by using excel program to extract the general equation for the force component in the tangential direction:

- Tangential force = $(5.3257 \times \text{dynamometer output}) + 16.701$

It should be noticed that when recording the readings of the dynamometer, the readings were nearly zero in the other force component. That means there is a negligible interaction between the two force directions.

Table 6. Calibration data for tangential.

Tangential force (Ft) calibration	
Applied force (N.)	Dynamometer output (micro strain)
50	5
100	15
150	25
200	35
250	45
300	55
350	65
400	70
450	80
500	90

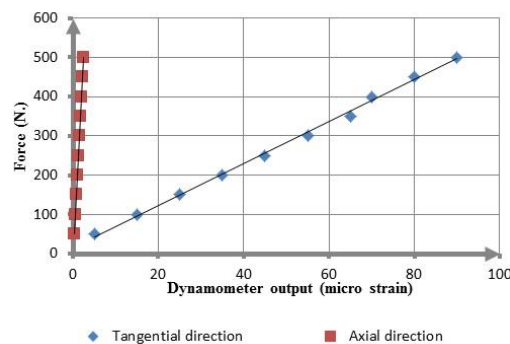


Fig. 11. Calibration data of tangential force.

International Journal of Innovative Research in Science, Engineering and Technology

(An ISO 3297: 2007 Certified Organization)

Vol. 6, Issue 8, August 2017

The tangential force measured by using dynamometer device is presented in Table 7. It is shown in Fig. 12 the proportionality relation between the feed rate and tangential force. When the feed rate increases the tangential force also increases. That's due to the increasing of the cutting area when the feed rate increases and that causes the cutting force to increase.

Table 7. Tangential force measurements from experimental work.

Feed (mm./rev)	Tangential force (N.)
0.12	363
0.15	416
0.18	480
0.2	523
0.22	560
0.26	629

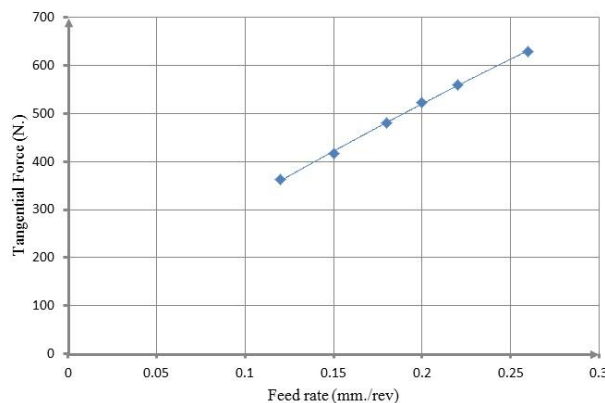


Fig. 12. Tangential forces for different feed rates.

Simulation Results and Comparison with Experimental Results

Proper selection of damage evolution value:

It is necessary to define the damage evolution criterion – element deletion criterion- for modeling a reliable cutting process. The damage evolution in Abaqus program is defined as the displacement that the element nodes move before failure. Some trials are held on Abaqus program to define the proper selection of the damage evolution value by comparing tangential force results. Table 8 shows the results of four values of the damage evolution for modeling the cutting process. The simulation results showed that the damage evolution value of 0.25 mm gives agreement with the experimental results for feed rates 0.15 and 0.26 mm/rev.

International Journal of Innovative Research in Science, Engineering and Technology

(An ISO 3297: 2007 Certified Organization)

Vol. 6, Issue 8, August 2017

Table 8. Tangential forces for different damage evolution values.

Damage Evolution (mm.)	Tangential forces			
	Simulation Model	Experimental	Simulation model	Experimental
	At feed rate =0.15 mm./rev	At feed rate =0.15 mm./rev.	At feed rate =0.26 mm/rev.	At feed rate =0.26 mm./rev.
0.1	313	416		629
0.2	386		588	
0.25 (proper choice)	401		632	
0.3	431		603	

Tangential forces extracted from Lagranigan model:

Table 9 shows the tangential forces from simulated model using Lagrangian formulation. As shown from tables the error percentage is (9.5% to 18.1%).

Table 9. Tangential forces extracted from Lagrangian model vs. experimental work.

Feed \ (mm./rev)	Tangential force results		
	I Error I%	Lagrangian model	Experimental work
		Tangential Force (N.)	Tangential Force (N.)
0.12	9.5	397	363
0.15	14.4	476	416
0.18	14.2	548	480
0.2	14.3	598	523
0.22	15.3	645	560
0.26	18.1	743	629

Tangential forces extracted from Arbitrary Lagranigan-Eulerian (ALE) model:

Table 10 shows the tangential forces extracted from simulation model by using ALE formulation. As shown from table the error percentage is (2.3% to 9.4%). The error percentage from Tables 9 and 10 shows that ALE readings are more accurate than Lagrangian readings.

Comparison study between the two models:

The two modeling techniques are compared together with the experimental data for:

- Deviation from experimental readings
- Readings stability of each technique
- Chip formation

International Journal of Innovative Research in Science, Engineering and Technology

(An ISO 3297: 2007 Certified Organization)

Vol. 6, Issue 8, August 2017

Table 10. Tangential forces from ALE model vs. experimental work.

Feed \ (mm./rev)	Tangential force results		
	ALE model Tangential Force (N.)	Experimental work Tangential Force (N.)	I Error I%
0.12	329	363	9.4
0.15	400	416	4
0.18	454	480	5.5
0.2	505	523	3.4
0.22	542	560	3.2
0.26	614	629	2.3

Results Deviation from Experimental Readings

From Table 10, the error percentage of the two models with the experimental data shows that the error using ALE technique is less than Lagrangian technique due to the adaptive meshing in ALE model and excessive distortion in Lagrangian model.

Fig. 13 shows the deviation between the tangential force readings that are extracted from the two models and the experimental readings. All the readings of ALE model results are closer to the experimental readings than Lagrangian model results. It is also clear from Fig. 13 that the force readings of Lagrangian model deviates more from the experimental readings as the feed rate increases. This confirms the concept of Lagrangian modeling that when the volume of the material needed to be separated from the model increases, the material points flow with the distorted mesh grid and the distortion accumulates and increases causing the force readings to be increased.

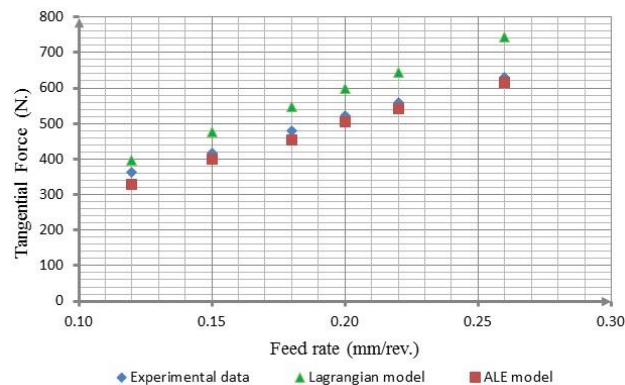


Fig. 13. Tangential force readings extracted from Lagrangian, ALE models and experimental work at different feed values.

International Journal of Innovative Research in Science, Engineering and Technology

(An ISO 3297: 2007 Certified Organization)

Vol. 6, Issue 8, August 2017

Stability of the Two Simulation Models

Stability of readings along the simulation time is a criterion for the efficiency of the model. Figs. 14 to 16 show the variation of the force readings extracted from the two models in comparison with the average values of the experimental readings for some feed rates. As shown from these figures, ALE model is more stable with time than Lagrangian model and the readings are more accurate. The reason for the instability of Lagrangian model is the accumulation of the distorted elements without deletion till failure occurred - damage evolution value is reached. After deletion, another group of elements is distorted and accumulated again due to the continuous penetration of the tool into the workpiece and more material points deform till failure. This causes the readings of the force to be unstable in form of increasing values when distortion is accumulated and decreasing values after elements deletion. But in case of ALE model, the adaptive meshing helps to keep the aspect ratio between the elements and the mesh grid adapt itself to prevent the excessive distortion of elements and give accurate force readings and stable readings with time.

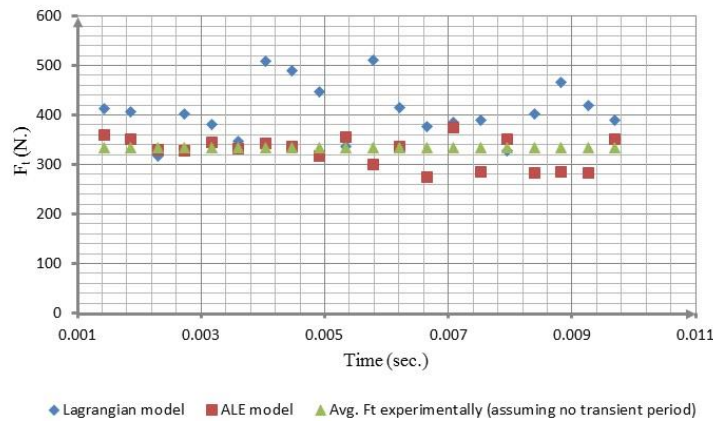


Fig. 14. Ft readings at feed rate = 0.12 mm/rev.

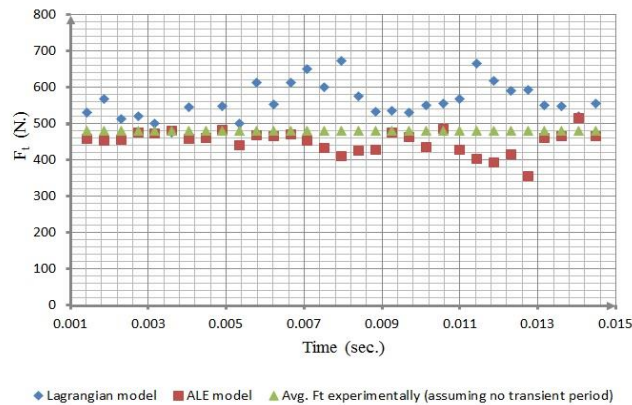


Fig. 15. Ft readings at feed rate= 0.18 mm/rev.

International Journal of Innovative Research in Science, Engineering and Technology

(An ISO 3297: 2007 Certified Organization)

Vol. 6, Issue 8, August 2017

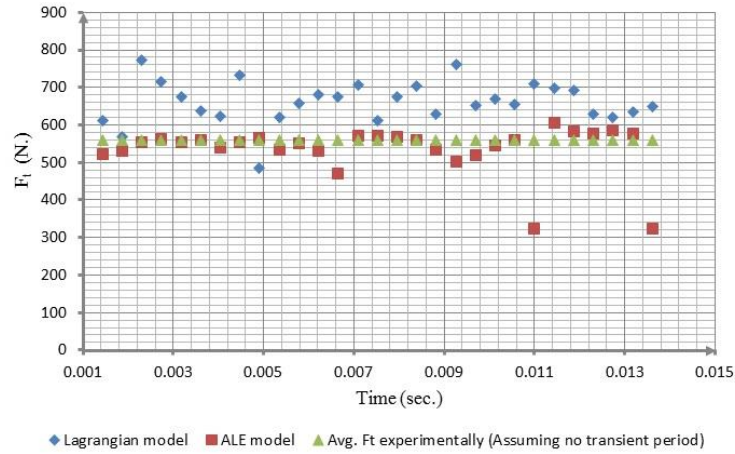


Fig. 16. Ft readings at feed rate = 0.22 mm/rev.

Chip Formation

Figs. 17 and 18 shows the chip formation in Lagrangian model and ALE model. As shown the excessive distortion is so clear in Lagrangian model but in ALE model, the adaptive mesh conserves the aspect ratio of the elements. ALE model shows a reliable form for the chip.

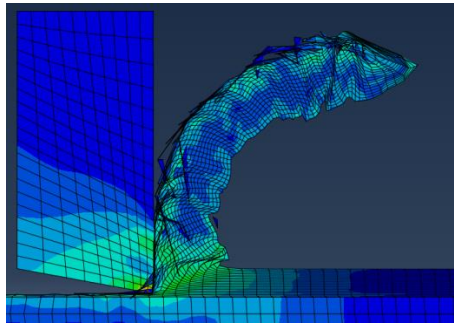


Fig. 17. Chip form in Lagrangian model.

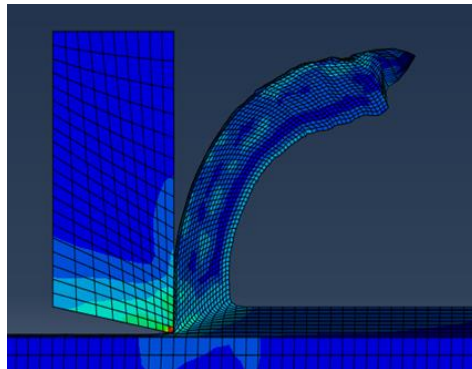


Fig. 18. Chip form in ALE model.

International Journal of Innovative Research in Science, Engineering and Technology

(An ISO 3297: 2007 Certified Organization)

Vol. 6, Issue 8, August 2017

IV. CONCLUSION

Finite element method is a powerful tool that can be utilized in many fields such as machining. This paper adopted FEM in one of the most important studies in machining which is orthogonal cutting simulation and cutting force prediction. Some points is concluded and presented in this paper:

1. Johnson-Cook model used for simulating the material behavior showing good agreements with the experimental results.
2. Chip separation is simulated using ABAQUS/CAE with defining the damage model and damage evolution criterion for workpiece. The damage evolution criterion is defined by choosing a proper value after trials of comparing the tangential forces extracted from the model with the experimental work to get the more suitable value for damage evolution.
3. Lagrangian model and ALE model were adapted for simulating the cutting process. Both models can simulate the cutting process and extract the cutting force with maximum error percentage 18.1% from Lagrangian model and 9.4% from ALE model.
4. The extracted results of tangential forces and chip form showed that ALE model is more accurate and stable than Lagrangian model. This is due to ALE model that depends on adaptive meshing technique and this mesh adaptation gives the elements the ability to deal with high deformation related to the cutting process as the mesh adapts itself according to the aspect ratio between elements to control any excessive distortion and converse its shape. But when using Lagrangian model, it doesn't control the excessive distortion due to deformation which causes the deviation of its results from the experimental results.

REFERENCES

- [1] P. Amrita , SK. Pal, AK Samantaray, "A Finite Element Study of Chip Formation Process in Orthogonal Machining ", International Journal of Manufacturing, Vol.1, pp. 19-45, 2011.
- [2] S.Jaspers , "Metal Cutting Mechanics and Material Behaviour", Ph.D., Technische Universiteit Eindhoven, Eindhoven, Netherlands,1999.
- [3] ABAQUS Theory Manual ver, vol. 6, no 14, 2014.
- [4] C. Kilikaslany, "Modeling and simulation of metal cutting by finite element method", Izmir Institute of Technology, Izmir, Turkey, 2009.
- [5] THC Childs, K. Maekawa, T. Obikawa, Y.Yamane, "Metal Machining Theory and Applications", Vol 10, 1st. edition, Elsevier Ltd, Linacre house, Jordan Hill, Oxford, 1999.
- [6] Fernell tools web site, 2015.
- [7] Kennametal catalog, Cutting recommendations for turning operation.
- [8] U. Silva, C. Diniz, S. Rocha, J. Filho, R. Pereira, A. Filho, P. Maia, "Finite Element Modeling for Orthogonal Cutting Process", SAE Technical Paper, 2015.
- [9] F. Salvatore, S. Saad, H. Hamdi, "Modeling and simulation of tool wear during the cutting process ", 14th CIRP Conference on Modeling of Machining Operations, Turin, Italy, 2013.
- [10] JD.Seidt, A. Gilat, JA.Klein, JR.Leach, " High Strain Rate, High Temperature Constitutive and Failure Models for EOD Impact Scenarios", Proceedings of the 2007 SEM annual conference and exposition on experimental and applied mechanics, Springfield, MA.